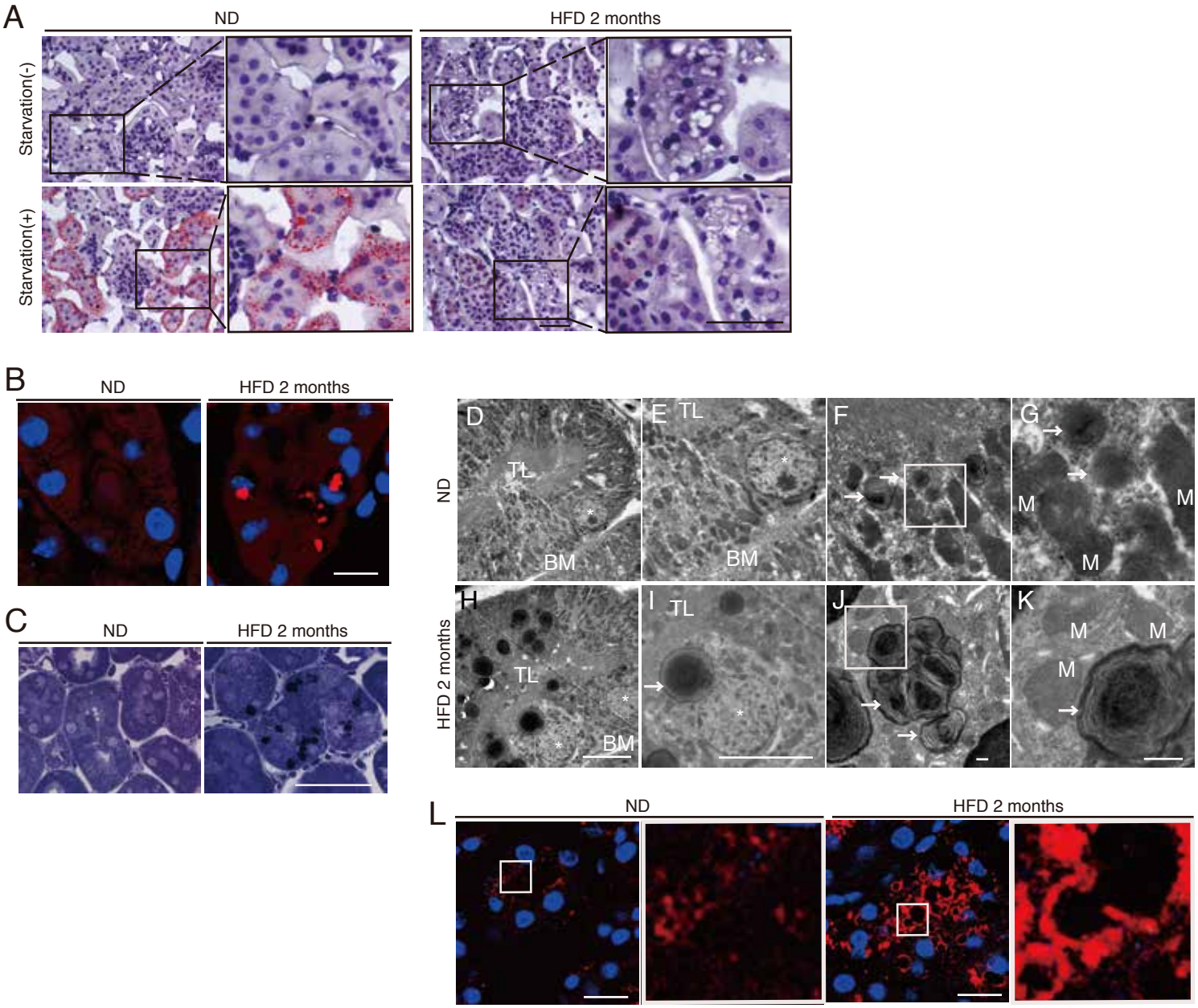

Supplementary Figure 1. HFD promotes phospholipid accumulation in the lysosome of the proximal tubules

(A) Oil Red O-stained kidney cortical regions of *nonobese* or *obese* mice that were either fed or subjected to 24 hours of starvation (n = 6-9 in each group). Counterstaining was performed with hematoxylin. (B and C) Nile red (B) and toluidine blue (C) stainings of the kidney cortical regions of *nonobese* or *obese* mice (n = 5 in each group). (D-K) Electron micrographs of *nonobese* (D-G) and *obese* mice (H-K) (n = 3 in each group). BM, basement membrane; TL, tubular lumen; M, mitochondria; arrow, lysosome, *, nucleus. Magnified images of lysosomes and mitochondria are presented. (L) Kidney sections were immunostained for LAMP1, a marker of lysosomes (red), and counterstained with DAPI (blue) (n = 5 in each group). Images are representative of multiple experiments. Bars: 50 μm (A and C), 10 μm (B, D, H, and L), and 500 nm (E-G and I-K). Values represent the mean ± SE. Statistically significant differences (*$P < 0.05$ vs. treatment-matched $Atg5^{F/F}$ control littermates; #$P < 0.05$ vs. *nonobese* mice) are indicated. F/F, $Atg5^{F/F}$ mice; F/F;KAP, $Atg5^{F/F}$;KAP mice.

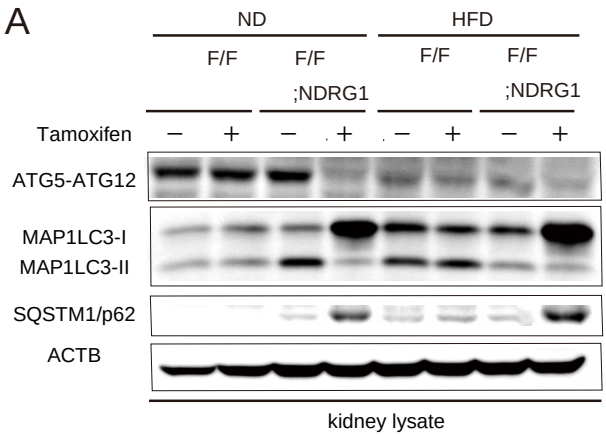
A
ND
HFD
F/F
F/F
;NDRG1
F/F
F/F
;NDRG1
Tamoxifen
– + – + – + – +
ATG5-ATG12
MAP1LC3-I
MAP1LC3-II
SQSTM1/p62
ACTB
kidney lysate

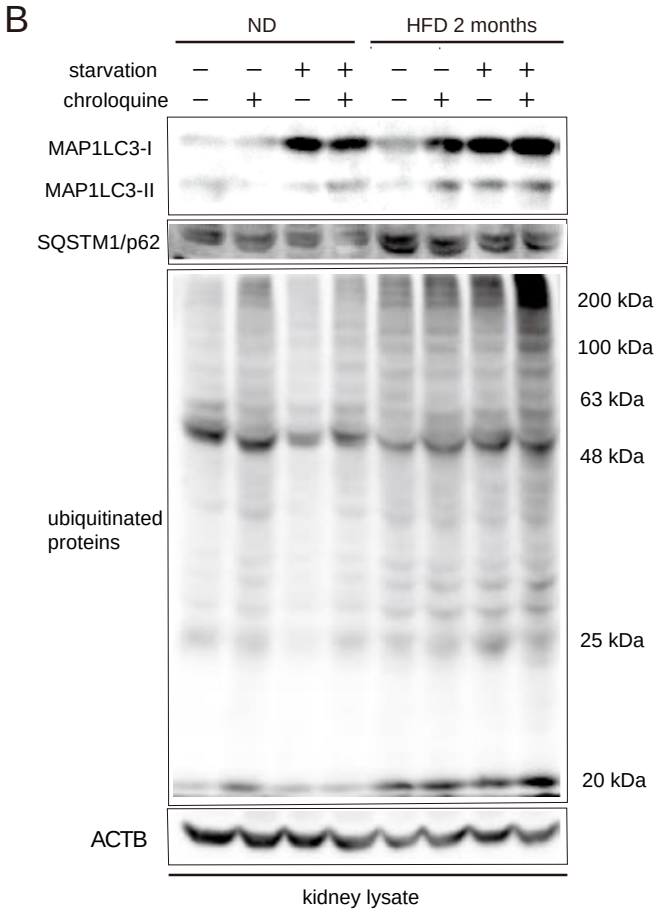
B
ND
HFD 2 months
starvation
chroloquine
– – + + – – + +
– + – + – + – +
MAP1LC3-I
MAP1LC3-II
SQSTM1/p62
ubiquitinated proteins
200 kDa
100 kDa
63 kDa
48 kDa
25 kDa
20 kDa
ACTB
kidney lysate

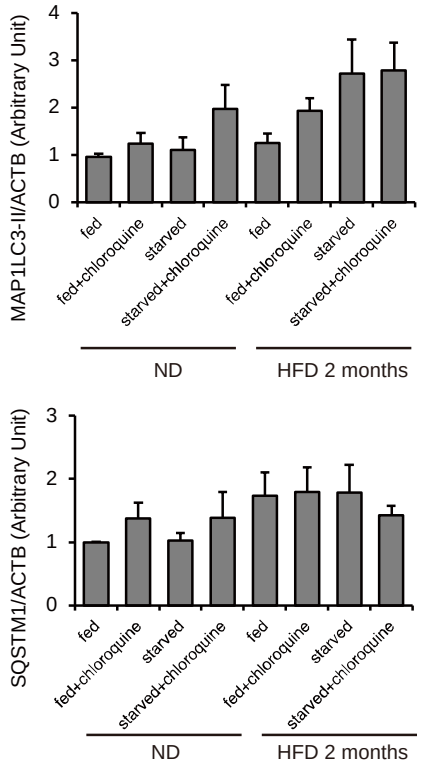
C
MAP1LC3-II/ACTB (Arbitrary Unit)
0
1
2
3
4
fed
fed+chloroquine
starved
starved+chloroquine
fed
fed+chloroquine
starved
starved+chloroquine
ND
HFD 2 months
SQSTM1/ACTB (Arbitrary Unit)
0
1
2
3
fed
fed+chloroquine
starved
starved+chloroquine
fed
fed+chloroquine
starved
starved+chloroquine
ND
HFD 2 months

Supplemental Figure 2. Western blot analysis using whole kidney lysates of *nonobese* or *obese Atg5$^{F/F}$*-NDRG1 and *Atg5$^{F/F}$* control mice, and GFP-MAP1LC3 transgenic mice
(A) Western blot analysis using whole kidney lysates of *nonobese* or *obese Atg5$^{F/F}$*-NDRG1 and *Atg5$^{F/F}$* control mice. Autophagy-deficiency was confirmed by the reduction of Atg5 expression, blockage of conversion of MAP1LC3-I to MAP1LC3-II, and the accumulation of SQSTM1/p62 in the kidney cortexes of *nonobese* or *obese Atg5$^{F/F}$*-NDRG1 mice treated with tamoxifen (n = 4 or 5 in each group). (B) Western blot analysis using whole kidney lysates of *nonobese* or *obese* GFP-MAP1LC3 transgenic mice that were either fed or subjected to 24 hours of starvation, with or without chloroquine administration (n = 6-9 in each group). A representative immunoblot (B) and quantification by densitometry (C) of HFD-mediated alterations in protein levels of MAP1LC3, SQSTM1/p62, and ubiquitinated proteins are shown. The mean value of fed young control mice without chloroquine administration was adjusted to "1" as a reference (C). Data are provided as mean ± SE. Statistically significant differences (*, $P < 0.05$) are indicated. ACTB was used as loading control. F/F, *Atg5$^{F/F}$* mice; F/F;NDRG1, *Atg5$^{F/F}$*-NDRG1 mice.

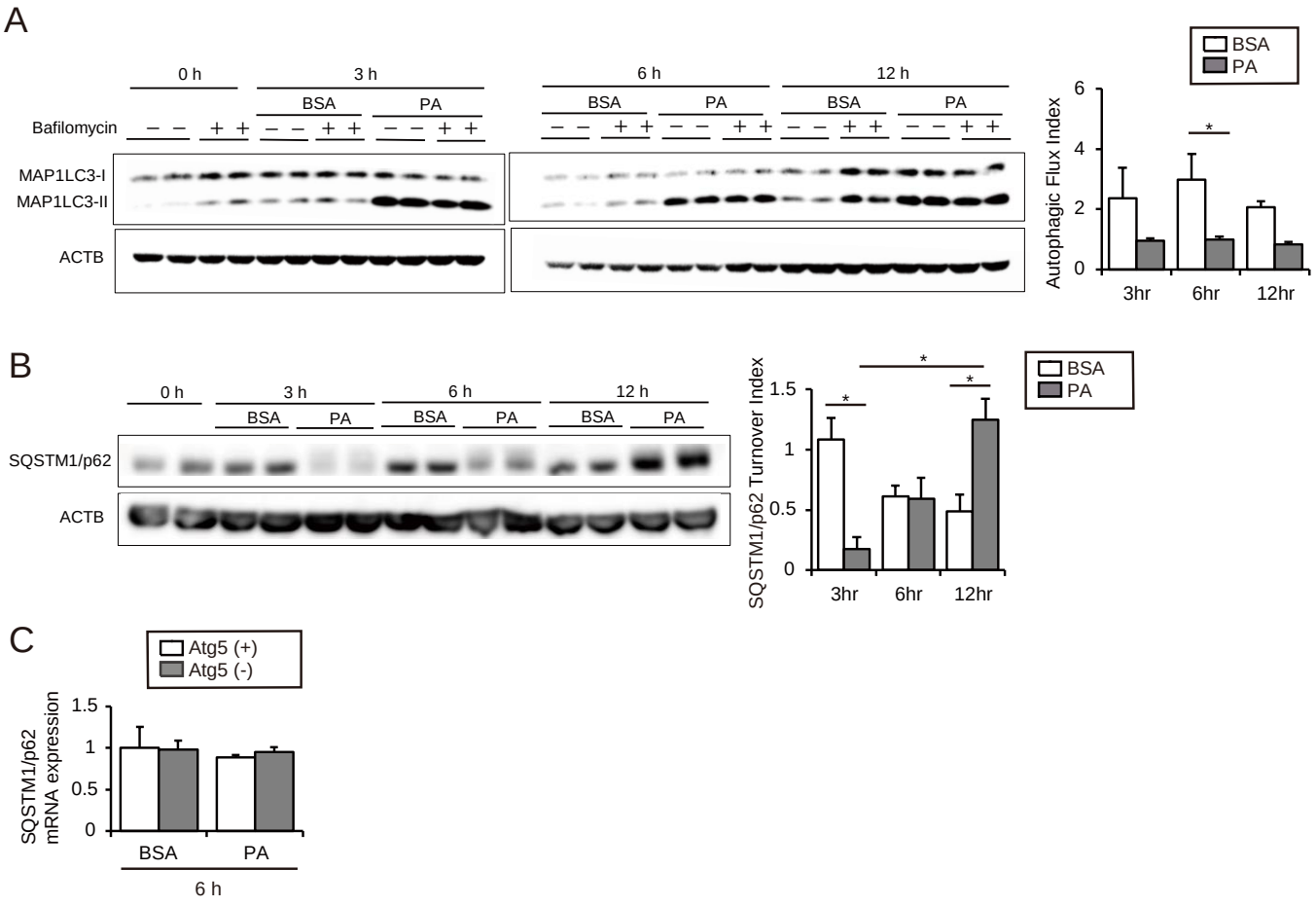

Supplementary Figure 3. PA affects autophagic activity in the PTCs

Autophagic flux in the PTCs during BSA or PA overload was estimated by the conversion from MAP1LC3-I to MAP1LC3-II as a readout of autophagosome formation and by the SQSTM1/p62 degradation assay at the indicated times (n = 4-5, respectively). (A and B) Western blot analysis of MAP1LC3 (A) and SQSTM1/p62 (B). Autophagic flux index (A) (defined as the proportion of the levels of MAP1LC3-II in the presence of bafilomycin A1 to the levels of MAP1LC3-II in the absence of bafilomycin A1) and SQSTM1/p62 turnover index (B) (defined as the proportion of the levels of SQSTM1/p62 of indicated sample to the levels of SQSTM1/p62 of untreated controls at the baseline) are shown. (C) Messenger RNA expression levels of SQSTM1/p62 were assessed in autophagy-competent and -deficient PTCs treated with either 0.25 % BSA or 0.25 mM PA for 6 hours (n = 3). All images are representative of multiple experiments. Data are provided as mean ± SE. Statistically significant differences (*$P < 0.05$) are indicated. Atg5(+), autophagy-competent PTC; Atg5(-), autophagy-deficient PTC.

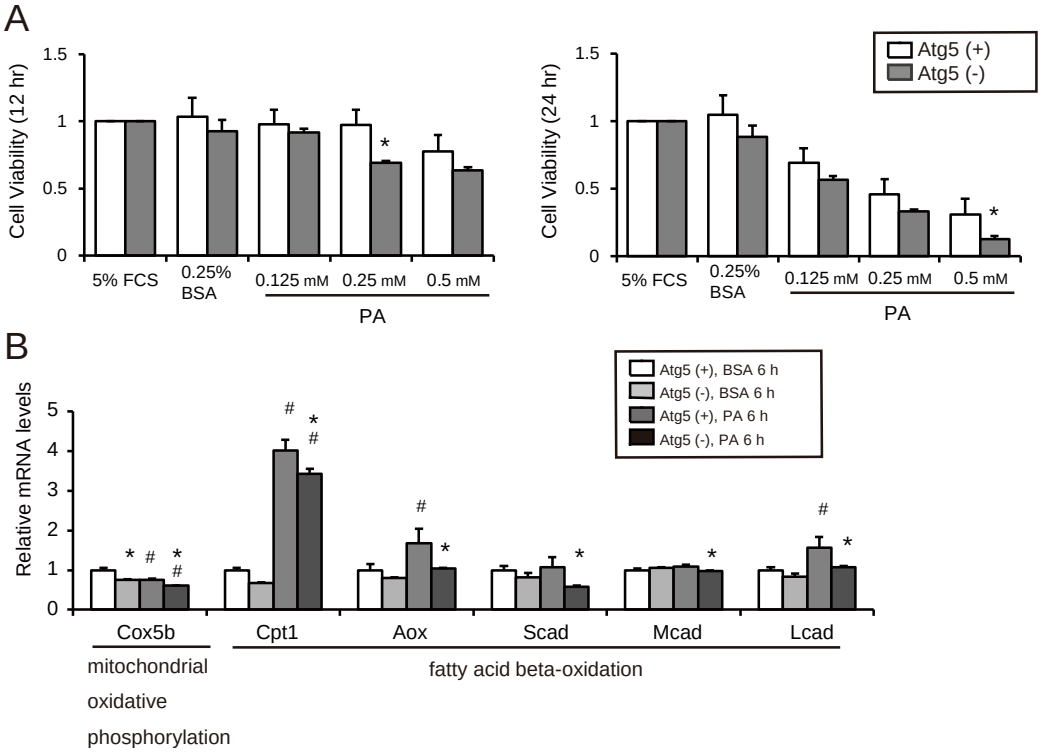

Supplementary Figure 4. Autophagy protects PTCs during PA overload
(A) Cell survival of autophagy-competent and -deficient PTCs incubated with the indicated concentrations of FBS, BSA, or PA for 12 or 24 hours. (B) Messenger RNA expression levels of mitochondrial oxidative phosphorylation-, and FA b-oxidation-genes were assessed in autophagy-competent and -deficient PTCs treated with either 0.25 % BSA or 0.25 mM PA for 6 hours (n = 6). Data are provided as mean ± SE. Statistically significant differences (*$P < 0.05$ vs. autophagy-competent cells of corresponding treatment; #$P < 0.05$ vs. BSA-treated control cells) are indicated. Atg5(+), autophagy-competent PTC; Atg5(-), autophagy-deficient PTC.

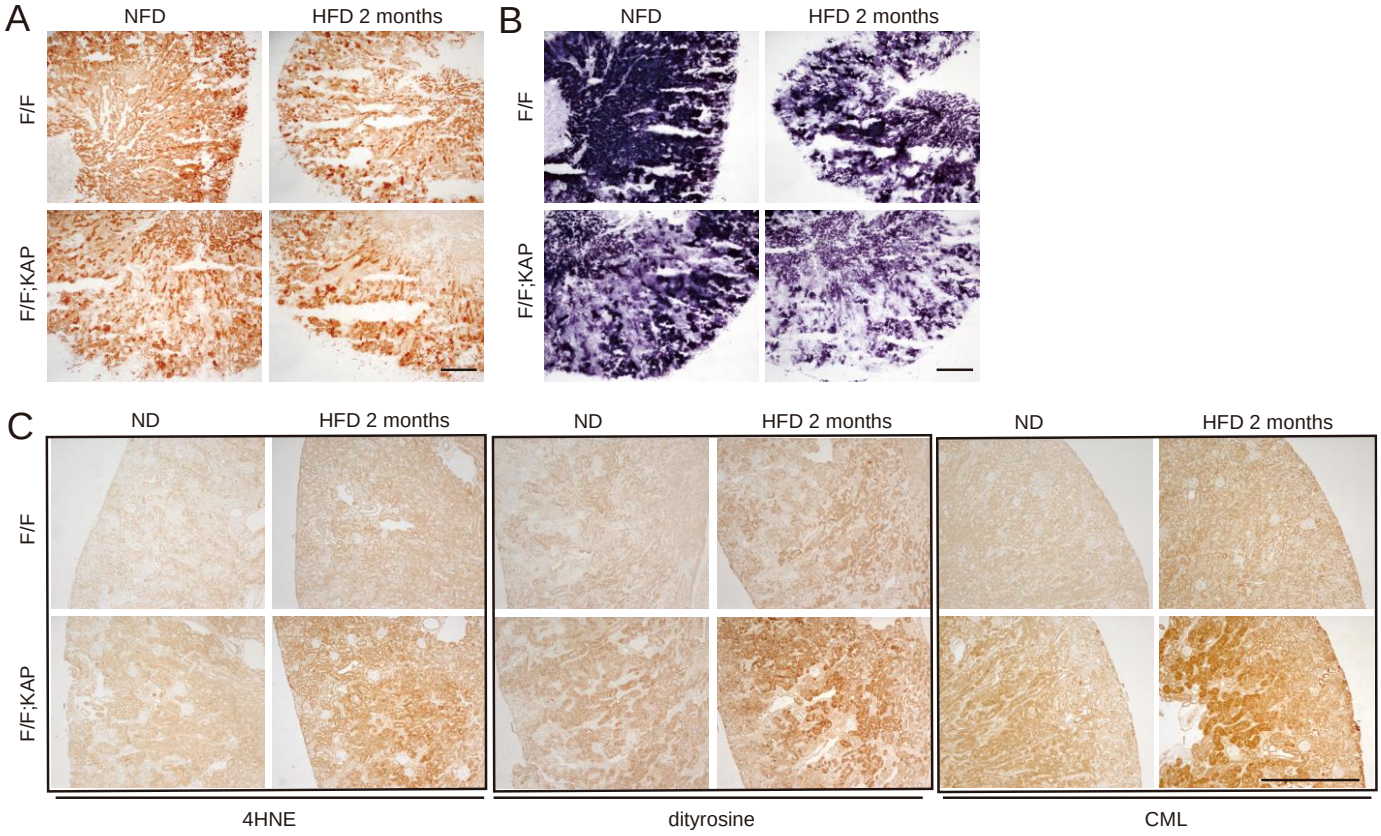

Supplementary Figure 5. Autophagy deficiency aggravates HFD-induced mitochondrial dysfunction

(A and B) Representative images of COX (A) and SDH (B) stainings and immunostaining of oxidative stress indicators, including 4-HNE, dityrosine, and CML (C) in the kidney cortical regions of *nonobese* and *obese* *Atg5*$^{F/F}$ and *Atg5*$^{F/F}$;KAP mice (n = 5 (A and B) and 7 (C) in each group). Bars: 500 μm. F/F, *Atg5*$^{F/F}$ mice; F/F;KAP, *Atg5*$^{F/F}$;KAP mice.

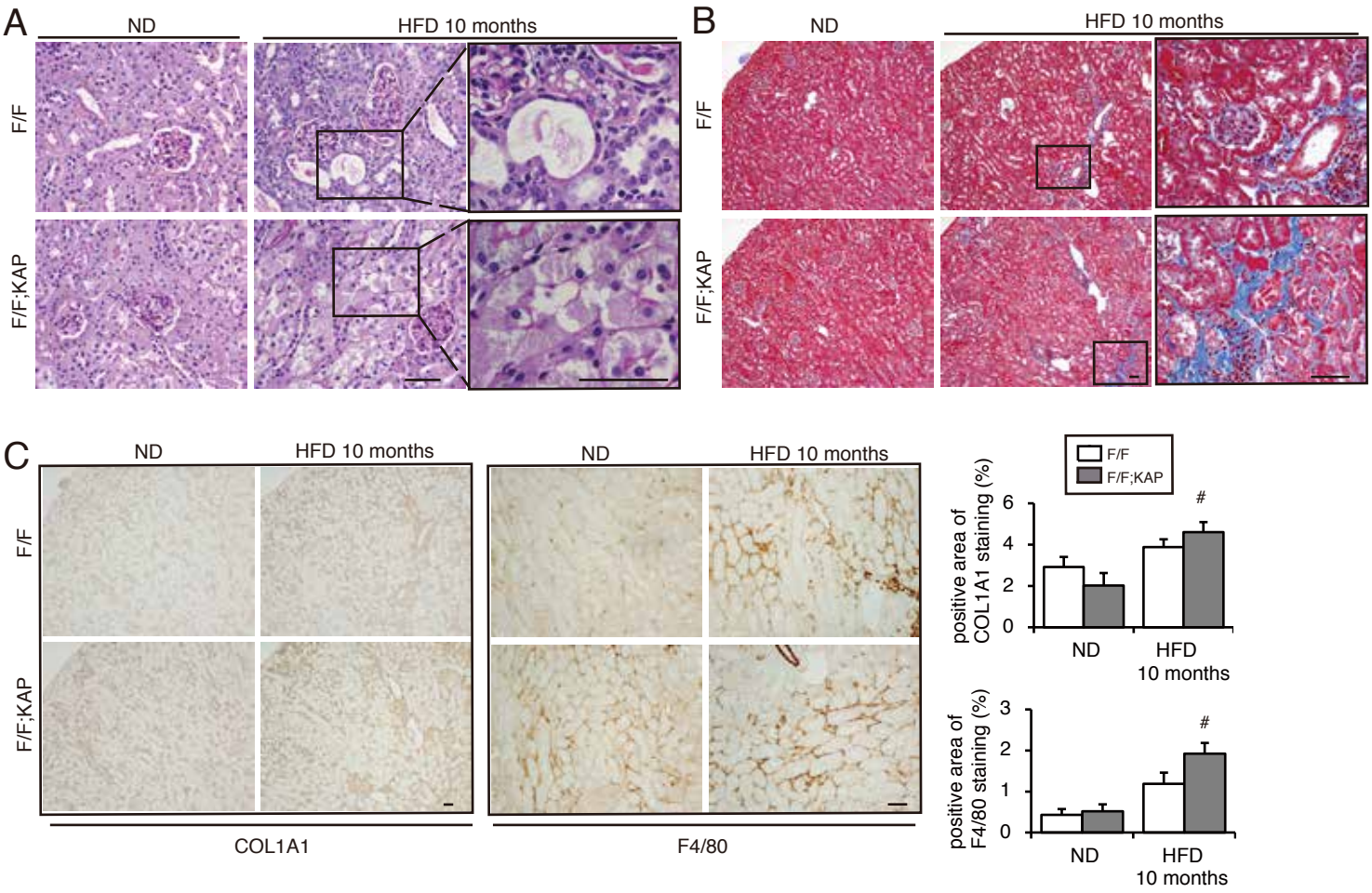

Supplementary Figure 6. Prolonged HFD induces macrophage infiltration and fibrosis in the autophagy-deficient kidney

(A-C) PAS-staining (A), Masson trichrome staining (B) and immunostaining for collagen type I and F4/80 (C) in kidney cortical regions of *Atg5*$^{F/F}$ and *Atg5*$^{F/F}$;KAP mice fed an HFD for up to 10 months (n = 7-10 in each group). (A) Magnified images from *obese* mice are presented. (C) The proportion of the immune-positive area for collagen type I and F4/80 was quantified in at least 10 high-power fields (× 400). All images are representative of multiple experiments. Bars: 50 μm. Values represent the mean ± SE. Statistically significant differences (*$P < 0.05$ vs. treatment-matched Atg5$^{F/F}$ control littermates; #$P < 0.05$ vs. nonobese mice) are indicated. F/F, *Atg5*$^{F/F}$ mice; F/F;KAP, *Atg5*$^{F/F}$;KAP mice.

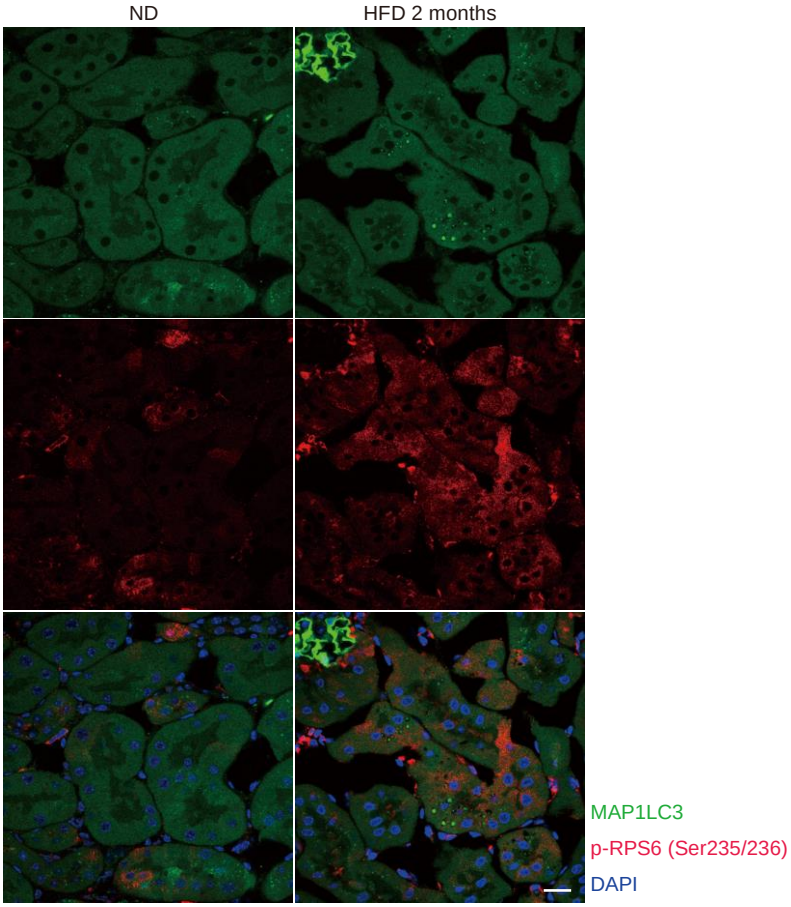

Supplemental Figure 7. Immunofluorescence analysis of p-RPS6 (Ser235/236), a marker for mTORC1 activation, in the kidney cortical regions of *nonobese* or *obese* GFP-MAP1LC3 transgenic mice

Relation between GFP-positive puncta formation and mTORC1 signal was assessed in the proximal tubules of *nonobese* or *obese* GFP-MAP1LC3 transgenic mice (n = 3). Kidney sections were immunostained for p-RPS6 (Ser235/236), a marker for mTORC1 activation and counterstained with DAPI (blue). Bar: 20 μm.

	No	BMI	Diagnosis	Age	Gender	Urinary protein excretion (g/day)	Serum creatinine (mg/dl)
obese patients (n=5)	1	30.4	Interstitial Nephritis	53	F	0.57	1.30
	2	31.2	IgA Nephrophathy	46	M	1.73	1.01
	3	39.7	FSGS	19	M	6.77	1.39
	4	33.6	Diabetic Nephropathy	57	F	5.49	0.86
	5	31.3	IgA Nephrophathy	42	F	4.62	0.87
nonobese patients (n=5)	6	24.4	IgA Nephrophathy	52	M	1.79	1.13
	7	20.2	MCNS	32	M	5.82	1.32
	8	21.5	MCNS	25	F	4.14	0.59
	9	24.0	Nephrosclerosis	49	M	4.42	1.99
	10	21.3	IgA Nephrophathy	33	F	0.55	0.58

Supplemental Table 1. Clinical characteristics of obese and nonobese patients
Clinical characteristics of obese and nonobese cases with chronic kidney diseases (n = 5, respectively) are shown. BMI, Body mass index; FSGS, focal segmental glomerulosclerosis; MCNS, minimal change nephrotic syndrome.